Hydrothermal Synthesis and Characterization of Cobalt Doped Bismuth Oxide NPs for Photocatalytic Degradation of Methyl Orange Dye

Ihsan Ghani[1], Muhammad Kashif[1], Osama Ali Khattak[2], Muffarih Shah[1], Shah Nawaz[3], Saif Ullah[1], Shafaq Murad[1], Saira Naz[1], Hina Wali Khan[1], Sheraz Muhammad[1*], Mansoor Jamal[1]

1. **Department of Chemistry, Abdul Wali Khan University, Mardan, KPK, Pakistan.**
2. **College of Chemistry and Chemical Engineering, Taiyuan Institute of Technology, China.**
3. **Department of Chemistry, Bacha Khan University Charsadda, KPK, Pakistan.**

*Corresponding Author- Sheraz Muhammad

Abstract

Bismuth oxide is the substance used in photocatalytic processes the most due to its excellent band structure and stability. It functions as the photo catalyst to degrade organic dyes like methyl orange and has a number of advantages as a catalyst. Purified BiO significant limitations that reduce its photocatalytic effectiveness, however. Dopant addition will thus improve its photocatalytic efficiency. Nitric acid, sodium hydroxide, cobalt nitrate, and bismuth nitrate are used to produce cobalt doped bismuth oxide nanoparticles. In order to create the necessary solution, sodium hydroxide was gradually added to a solution containing the nitrate of bismuth and cobalt nitrate till the pH value reached 4, which is the point at which the most precipitate is likely to form. After that, the mixture was put into a Teflon autoclave at 150°C for hydrothermal synthesis. The solution is then dried at 80°C after being rinsed with deionized water. The leftover material was then pulverized and calcined at 450°C in a muffle oven. The resulting particles were characterized utilizing a variety of methods, such as Uv-visible spectroscopy, FT-IR spectroscopy, XRD, EDX along with SEM. Using an UV-Vis, the absorbance of 2, 3 and 4 percent Co/BiO NPs with various Co concentrations be determined at the range of 292 nm, 303 nm and 310 nm each. The functional groups of cobalt-doped bismuth oxide nanoparticles were studied using FT-IR spectroscopy. The Co/BiO bond generated a signal in 883 cm^{-1}, whereas the maximum range of BiO stretch was 454 cm^{-1}. SEM Images of Co/BiO NPs be later put through

to detailed investigation using a scanning electron microscope (SEM) at different magnifications. In the presence of cobalt, it was revealed that the diameters of Co/BiO NPs were 44.44 nm, 49.53 nm, & 50.41 nm at concentrations of 2%, 3%, & 4% respectively. This was accomplished with the use of Sherrer's equation, which also helped to establish the average crystalline structure of cobalt doped BiO. The activity of the produced NPs was examined for MO degradation under sun illumination. The 3Co/BiO photo-catalyst degraded more than 94% of the MO dye, whereas the 2Co/BiO nanoparticles and the 4Co/BiO nanoparticles each degraded roughly 93.04% and 92.72% of the MO dye, respectively, according to the findings of the photocatalytic activity.

Keywords; Hydrothermal Synthesis, Cobalt doped Bismuth Oxide, Nanoparticles, Photocatalysts, Characterizations, MO Dye Degradation,

1. Introduction

The field of nanotechnology has drawn a lot of interest over the years. The most crucial part of the nanotechnologies is the nanoparticles themselves. Nanoparticles, which can be composed of metals, oxides of metal, the element carbon, or organic substances, are incredibly small particles with sizes ranging from 1 nm to 100 nm [1-3]. When in comparison to their respective larger scale counterparts, the nanoparticles exhibit unique chemical, biological, and physical characteristics that are more prominent at the nano-scale. This phenomenon results from a significant increase in surface area relative to volume, an improvement in reaction or stabilization during a chemical reaction, a rise in mechanical strength, and other factors. These qualities have led to the use of nanoparticles in a wide range of implementations [4]. Nano-particles might also be obtained from the nature as well as being produced as a result of human activity. Due to their sub microscopic size, they display various material properties. In a variety of fields, including engineering, medicine, environmental remediation, and photocatalysis, artificially produced nanoparticles may find practical applications [5].

The removal of environmental pollutants, the creation of energy, & the conversion of photon into chemical energy are just a few of the many uses for photo catalysis [6], the subject matter is crucial. Photocatalysis is a phenomenon that happens after photogenerated charge carriers scatter to the outer layer to start chemical reactions called redox reactions [7]. Majority of photocatalyst that are semiconductor oxides possess a wide band gap, they are only functional inside ultra

violet light. Because they can only use 3-5% of solar radiation in the visible spectrum, this restricts their usage in industrial applications. Because of relatively increased rate of recombination of electron-hole pairs, the efficiency of photo-catalytic reaction is low [8]. One of the most crucial elements required for enhancing the photo-catalytic efficiency of a semi-conductor photo catalyst, is the separation of photo-generated charge carriers. Consequently, in order to increase photocatalytic activity and improve performance, efficient surface traps are required to reduce the rate of separation of charge carriers as well as to decrease recombination rate. Therefore, in a need to improve the photo catalytic effectiveness of semiconductors, scientists are focusing on developing visible light active photo-catalysts. This can be done in one of two ways: either large band gap semi-conductors can be doped to attract charge carriers or by finding new semi-conductors with smaller band gaps to add more significance and more effectiveness to their usage in practice. Numerous oxide semiconductors were heavily utilized as photo-catalysts which include TiO_2, SnO_2, CdS, ZnO, and Bi_2O_3 [9-15]. On the other hand, the limitation of having an elevated photo-induced electron-hole rate of recombination makes these semiconductors struggle [16, 17]. A great deal of study and innovation has gone into adding the proper traps to surface of photo-catlyst. It is typically done by doping the surface of fundamental or bulk photo-catalyst using metallic or non-metallic ions, which causes heterostructures to form [18, 19]. The photocatalyic semiconductors TiO_2, ZnO, WO_3, Bi_2O_3, and CdS have all undergone extensive research [20, 21]. Bismuth oxide is a versatile material that can be used in a variety of applications, such as gas sensors, catalysts, and semiconductors. Bismuth oxide is occasionally used as a component in paints. Additionally, the use of tin catalysts containing bismuth may increase the degree of oxidation of isobutene [22]. The discovery of bismuth oxide as a new element took place in the 18th century. Bismuth oxide is a significant class semiconductor made of metal oxide with outstanding optical and electrical properties. These characteristics include high refractive index, photoconductivity, dielectric permittivity, and a wide band gap [23]. This has led to its widespread application in a variety of fields, including photo electric substances, sensors for gases, photocatalysis, functional ceramics & fuel cells made of metal oxide [24-28]. When creating Bismuth Oxide nanoparticles, one of three techniques may be used. These techniques include the hydrothermal, sol-gel, and combustion approaches [29-31]. Because of its distinctive structural features and physical characteristics, such as a high oxygen-ion conductance, thermally stable dielectric properties, and a high

refractive index, a p-type bismuth oxide heterogeneous semiconductor was thought to be one of the most effective photo catalysts and essential in the development of modern solid state technology. This was because it was regarded as one of the best and most powerful photo catalysts. This was because it's among the few semiconductors with these qualities. Bismuth oxide, which is inert to neutral water and has a visible band gap energy of 2.8 eV, can oxidize water to produce species with high reactivity, which can then be used to start a process of oxidation in the decomposition gases, dyes as well as chemicals used in pharmaceutical industry [32, 33]. Solid Oxide fuel cells and other types of fuel cell technology can use the highly ionic conducting electrolyte material known as bismuth oxide [34]. In solid oxide fuel cells, this material is present. Bismuth oxide is a superior oxide ion conductor due to the high ratio of oxygen vacancies in the material. Due to their capacity to transform chemical energy into electrical energy, oxygen vacancies are responsible for this. In addition to high-temperature oxygen pumps, this in based electrolyte conductor is utilized in various types of gas sensors [7]. However, due to the rapid recombination of charge carriers, photocorrosion, changes in structure, and creation of bismuth carbonate, (Bi_2O_2) CO_3, in the process of photocatalysis, the photo-catalytic effectiveness of bare Bismuth Oxide is not as better as was described [35]. As a result, bismuth oxide in its pure form is ineffective as a photocatalyst [36, 37]. Doping pure bismuth oxide with Rare Earth Metal and Transition metal oxides like Nb_2O_5, Ta_2O_5, and WO_3 can increase the photocatalytic efficiency of the material by separating the electron hole pairs and ultimately increasing the photocatalyst's light feedback. To achieve this, the photocatalyst's light response can be increased [38-43]. It might be accomplished by incorporating transition metal Oxides, Metal Oxides and Rare Earth Oxides into the Lattice. Furthermore, in the literature a few of the studies on metal-doped bismuth oxide have been done are described. Researchers predicted that a specific f electron orbital in rare earth metal ions would allow ions to speed up the incorporation of photo generated pairs of electrons and holes which takes place in the process of photo-catalysis [7, 44, 45].

In this work, we describe a simple hydrothermal method for producing cobalt co-doped bismuth oxide nanoparticles. After the production of the photo catalysts, they were analysed using conventional analytical techniques that include UV-Vis, FTIR, XRD, and SEM. When exposed to solar light, it was found that the synthesized nanomaterial was functional. Researchers were able to calculate the photocatalytic efficiency of the produced photo catalyst by using the Azo

MO dye's breakdown in an aqueous solution in response to light as a measure of the quantity of irradiation.

2. Experimental Methodology

Table 1: Apparatus Used in Hydrothermal Synthesis

Apparatus	Quantity
Autoclave	1
Magnetic Stirrer	1
Ultrasonic Bath	1
pH Meter	1
Centrifuge Machine	1
Oven	1
Analytical Balance	1
Glass Beakers	Multiple
Glass Pipettes	Multiple
Glass Stir Bars	Multiple

Table 2: Materials and Chemicals Used in Hydrothermal Synthesis

Material/Chemical	Purity	Supplier
Bismuth Nitrate Pentahydrate (Bi(NO3)3.5H2O)	99%	Sigma-Aldrich

Material/Chemical	Purity	Supplier
Cobalt Nitrate Hexahydrate (Co(NO3)2.6H2O)	99%	Sigma-Aldrich
Sodium Hydroxide (NaOH)	99%	Sigma-Aldrich
Methyl Orange Dye (MO)	Grade	Sigma-Aldrich
Ethanol (C2H5OH)	Analytical grade	Merck
Deionized Water	NA	Own Lab preparation

2.1.　　Synthesis of Cobalt doped Bismuth oxide NPs

The formation of cobalt-doped bismuth oxide was accomplished by hydrothermal synthesis. The hydrothermal production of cobalt-doped bismuth oxide nanoparticles is briefly described below. First, sodium hydroxide [NaOH], cobalt nitrate [Co $(NO_3)_2 \cdot 6H_2O$], and bismuth nitrate pentahydrate [Bi $(NO_3)_3 \cdot 5H_2O$] were employed as the starting ingredients for the synthesis. Under steady stirring, they were dissolved in deionized water to create a homogenous solution. The initial ingredients' molar ratio was held constant at 97:03 for Bi:Co. After that, the solution was put into an autoclave lined with Teflon and heated for 9 hours at 150°C. The precursors underwent hydrolysis throughout this process, and nucleation resulted in the formation of cobalt-doped bismuth oxide nanoparticles showed in fig 1. The produced nanoparticles were recovered by centrifugation after hydrothermal treatment and repeatedly rinsed with deionized water and ethanol to eliminate any remaining contaminants. The nanoparticles were then dried for several hours at a temperature of 80°C. Various methods, including X-ray diffraction (XRD), Scanning electron microscopy (SEM), FTIR spectroscopy and UV-Visible spectroscopy, were used to analyze the produced nanoparticles. Cobalt-doped bismuth oxide nanoparticles with a crystalline structure were formed, according to XRD measurements. The produced nanoparticles were spherical in form and had an average particle size of 20–30 nm, according to SEM and XRD examination. The nanoparticles demonstrated a significant UV absorption, which indicated their potential for photocatalytic applications, according to UV-Vis spectroscopy.
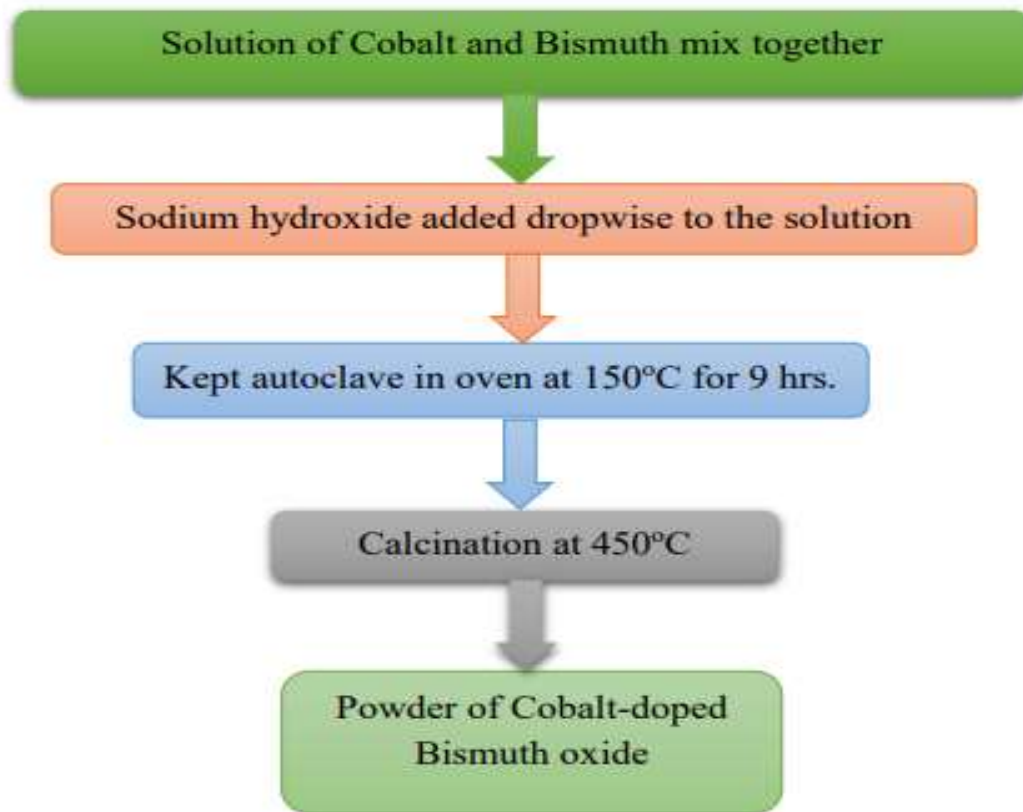
Figure 1. Preparation of Co/BiO NPs.

2.2.   Characterizations

The characterization approach was used to investigate the sizes, morphologies, and shapes of the prepared NPs. Using a computer-controlled JASCO V-650, the spectral behaviour of UV-Vis materials was investigated. A Nicolet 6700 FTIR analyzer was used to conduct an FTIR analysis in the range of 4500-400 cm^{-1} in order to identify the functional groups that were present in the samples (USA). The crystallization of the samples that were produced were assessed using X-ray diffraction. The device was used for XRD analysis (Bruker D8 Advance x-ray diffractometer). Using a Hitachi S-3500N scanning electron microscope (SEM), surface image measurements and chemical characterization of a material were performed.

2.3.   Photocatalytic degradation of Methyl Orange dye

The MO dye's photocatalytic degradation, which occurs when it is exposed to light, has been utilized to examine the photocatalytic effectiveness of the samples of NPs that were chemically synthesised. A light source (100V) was used to efficiently complete the photocatalytic reaction. 100 mL of dye solution containing 5 ppm of dye were mixed with 0.2 gram of catalysts in total. MO was present in the solution at a final concentration of 5 ppm. The suspension seen above was shook in the dark for 30 minutes at what was thought to be ambient temperature. This was carried out to bring the processes of adsorption and desorption into balance. When that was done, the mixture was quickly agitated and then subjected to ionizing radiation. This went on until the desired outcomes were obtained. Approximately 5mL of the solution were taken out at regular intervals and centrifuged to make sure the solid photo catalyst was effectively removed from the mixture. At some point during the experiment, a UV visible spectrometer was used to quantify the photo catalyst's MO adsorption capacity and how well it degraded the dye. Utilizing the stated formula, it was possible to measure the quantities of MO that were eliminated:

$$\text{Degradation efficiency (\%)} = Co - C/Co \times 100$$

3. Result and Discussion

In addition to studying the optical properties of enhanced doped BiO NPs, this study also looked at their structural and morphological characteristics, using a variety of experimental methods. The photocatalytic breakdown of MO dye was then carried out in the presence of light in order to investigate the photocatalytic activity of the NPs that had been generated. This was carried out in order to evaluate the outcomes.

3.1.   UV-Visible Spectroscopy

UV-Visible characterization, a low-cost, rapid, and straightforward characterization method, is widely used in the research of NPs. A useful technique for studying metal NPs is UV-Vis spectroscopy, which is sensitive to the accumulation state, refractive index, shapes, concentrations of substances, and sizes when they are close to the surface. Using UV-vis

spectroscopy, the crystalline and homogeneous nature of the cobalt-enriched BiO Nanopowder was examined. Investigations were also conducted on the Nano powder's visual properties. The UV-vis band of the produced nanopowder may be seen in Figure below. This band, which ranged from 240 nm to 600 nm, was gathered. In nanoparticles with 2%, 3%, and 4% cobalt doping in bismuth oxide, there is, respectively, a large exciton absorbance band at 293 nm, 303 nm, and 310 nm shown in fig 2. This supports the relevance of the surface shape theory, which controls the size of particles and the purity and is affected by these wavelengths. Making cobalt-enriched bismuth oxide involves a number of processes, one of which is the growth of monodispersed colloidal particles. Another result of this phase, which may also be its end, is the advent of quantum size effects. Band gaps of 2%, 3%, and 4% cobalt-doped bismuth oxide nanoparticles were discovered to be 4.09 eV, 3.96 eV, and 3.87 eV, respectively. These investigations clearly demonstrated that as the cobalt concentration in the sample rises, the band gap energies of doped bismuth oxide nanoparticles decrease over time. This greatly reduces the photocatalytic activity of nanoparticles made of bismuth oxide.
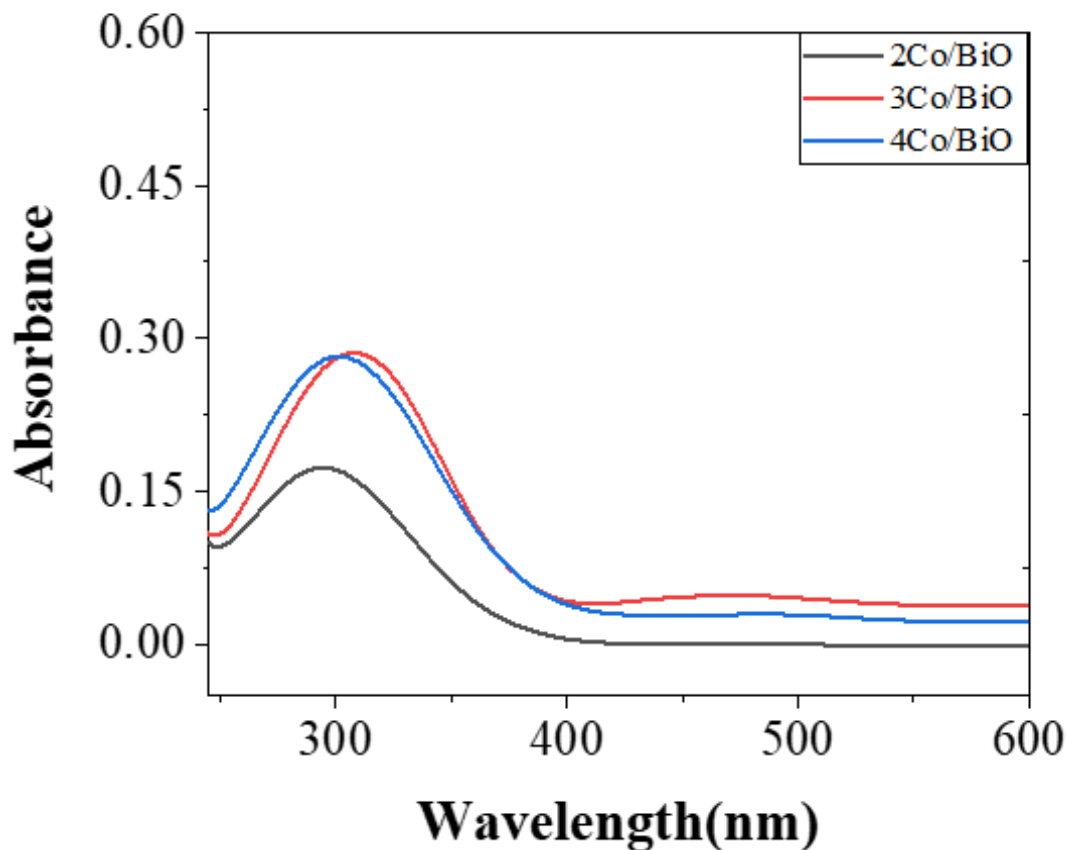
Figure 2. UV-Vis Absorption Cobalt doped Bismuth Oxide

3.2.   FT-IR Spectroscopy

FT-IR is an abbreviation for the technique known as Fourier transforms infrared spectroscopy, which is a method that may be used to test material samples to determine whether or not they contain functional groups. This may be accomplished in a number of different ways. Examining the infrared radiation that is emitted by the sample is the method used to do this. A confirmation of this sort may be performed in order to ascertain whether or not a substance has functional groups. This technique is very helpful for qualitative analysis because the infrared spectra's peak intensity can easily be used to identify the component's surroundings. Consequently, this technique is especially good for determining whether or not a component is present. This technique is used so frequently because of the aforementioned benefits. This characteristic makes it possible to instantly determine the nature of the element by use the spectrum's peak intensity as a reference point. The results of the FTIR spectrum taken between 4000 cm^{-1} and 400 cm^{-1} for 2%, 3% and 4% cobalt-doped Bismuth Oxide nanoparticles are shown in fig 3. The infrared bands ranges from around 3200 cm^{-1} -3400 cm^{-1} are caused by a similar elongation of the hydroxyl (OH) group. The distinctive oscillation mode of the NO_3 group can be observed between 1376 and 1450 cm^{-1} and is characterized by a broad peak that emerges at 454 cm^{-1} and an absorption band that can be seen at 883 cm^{-1}. Both of these features are associated with the BiO bond.
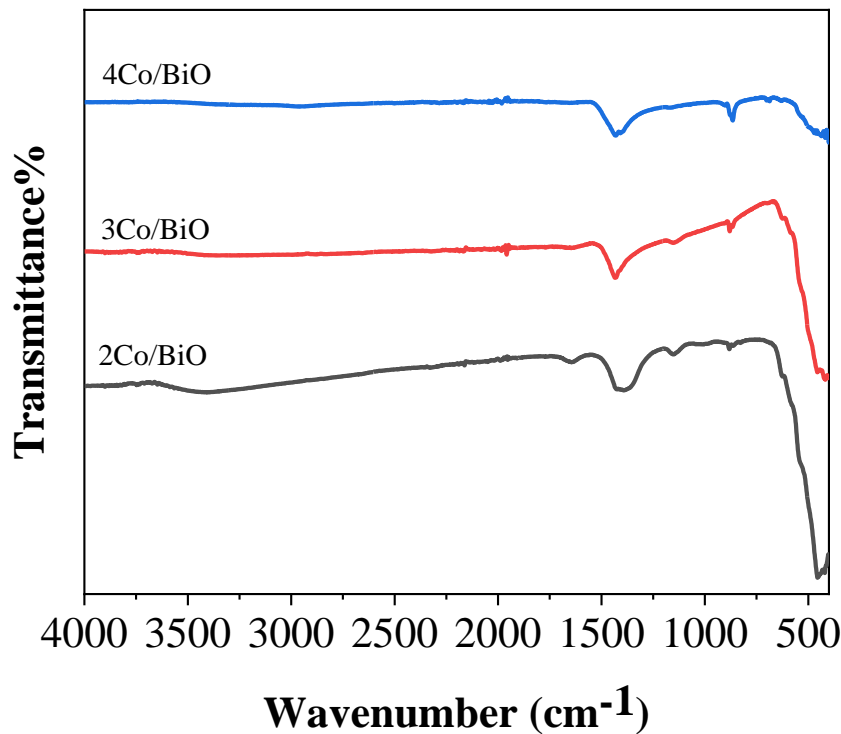
Figure 3. FT-IR analysis of 2%, 3% and 4% Cobalt Doped Bismuth oxide

3.3.   XRD Analysis

The process known as X-ray diffraction, or XRD, is particularly helpful for gathering information on crystalline solids since it doesn't harm the material. In addition to other structural information such as nature of crystalline, flaws and size of grain the XRD is utilized through deterring best phases, crystalline alignment, or even structures. Also the XRD analysis of Co/BiO Nps at different dopant ratios was studied to determine phase structure. Rather than XRD analysis of Co/BiO Nps is shown in Figure below as an illustration of a typical circumstance. The Co/BiO Nps exhibit nine XRD peaks that are clear and prominent at the following angles 2 theta = 25.7, 26.3, 27.2, 29.1, 32.8, 45.3, 46.2, 48.5, and 54.7. When compared to their respective crystal surfaces, their peaks are (012), (201), (102), (210), (112), (203), (129), (320), and (226). This research established the archetypal crystallite size of Co/BiO NPs to be 44.44 nm, 49.53 nm, and 50.41 nm at 2%, 3%, and 4% concentrations, respectively shown in fig 4. This conclusion

was reached using Scherer's methodology. The average crystallite diameter of Co/BiO NPs grows as the quantity of dopant increases and the peak strength declines. Also the rather narrow and distinct XRD peaks hint that the samples may represent an uncommon crystalline nanomaterial. This also demonstrates the instances of cobalt-doped bismuth oxide nanoparticles having a high degree of crystallinity.
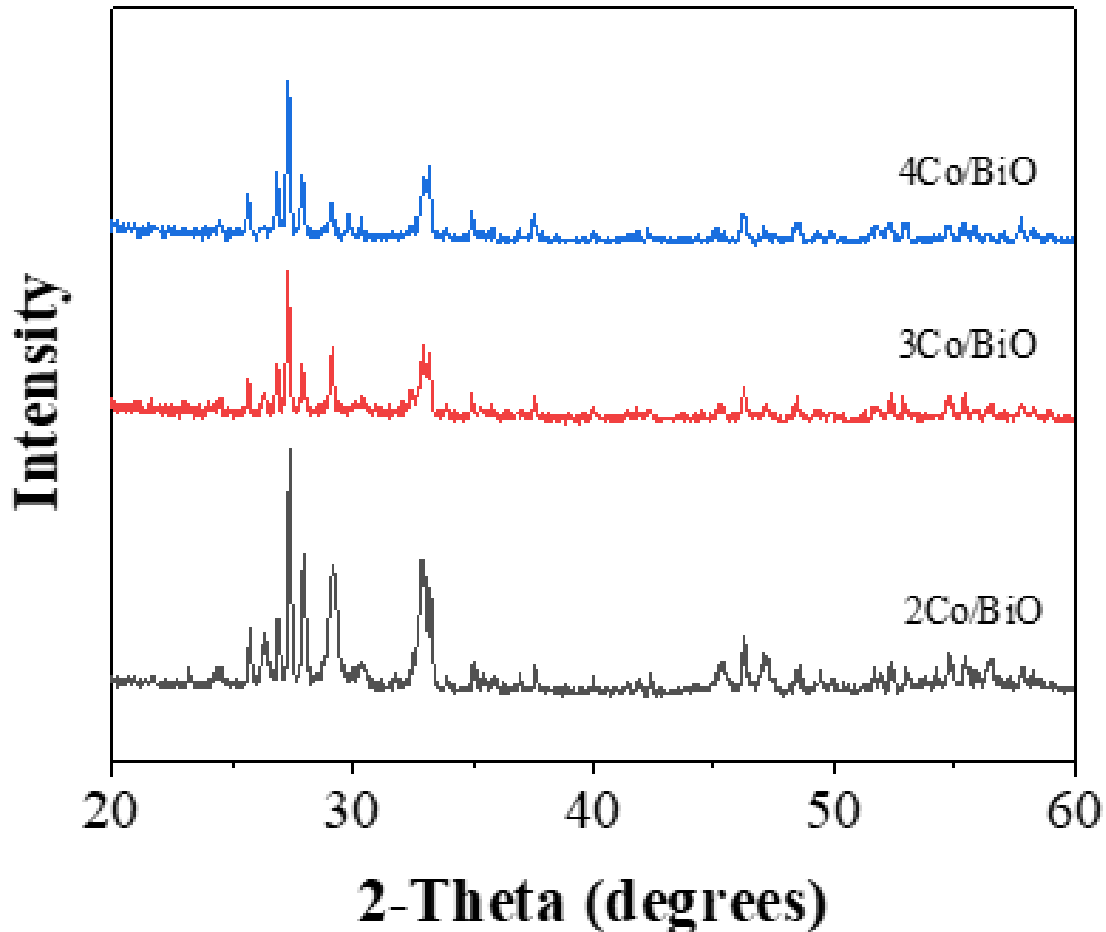

Figure 4. XRD analysis of 2, 3 and 4% of Co/BiO NPs

3.4.   Scanning Electron Microscope Investigation

Cobalt-doped bismuth oxide nanoparticles were produced and SEM was used to determine their dimensions and form. One can suggest that the particles were probably accumulated, asymmetrical, round in shape and the size is around 40-60 nm when the results of Scherrer's formulas for X-ray diffraction are analyzed collectively. This outcome is showed in fig 5 below.

The results of earlier research are confirmed by the SEM microscopy, which gives unambiguous proof that the nanostrips of lower cobalt dopant concentrations have a smooth texture. Additionally, the sample's agglomeration dramatically reduces as the amount of cobalt dopant rises. Interaction and attraction of the functional groups in the aqueous solution causes the particles to expand in size. The time spent blending the mixture may have an impact on the final particle size in addition to the ratios of the reduction agent to the saline solution. The appearance of agglomeration in some particles has been explained by the creation of hydrogen bonds among molecules in the surroundings of particles.
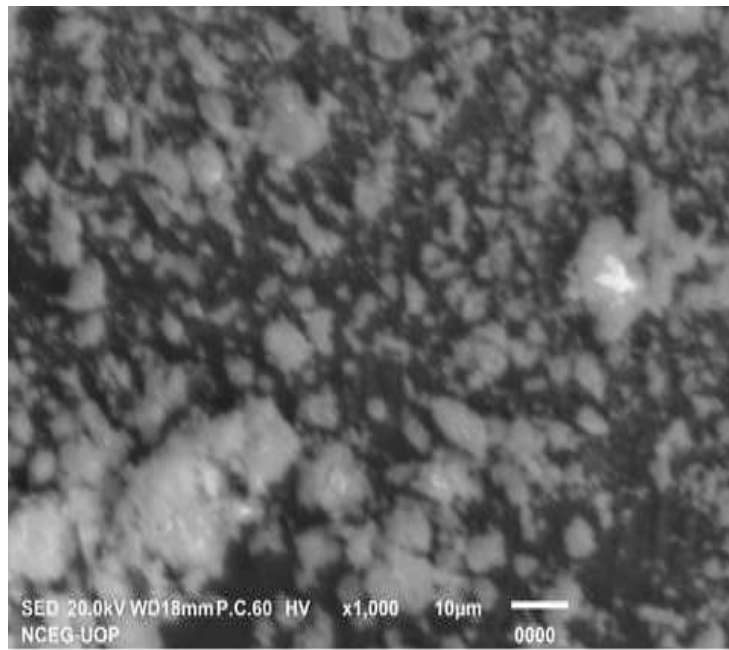

Figure 5. SEM image of 3% Co/BiO NPs

3.5.   **Photocatalytic Degradation**

When a material absorbs an amount of light energy equal to or greater than its bandgap energy, it begins to exhibit photocatalytic activity. It is necessary for this activity to take place. The possibility exists if the substance in question is a semiconductor. As a direct consequence of this, the system is saturated with energy that is distributed between its electrons and its holes. It is

possible for adsorbed reactants to interact with the electron-hole pair as a result of their transit to the surface, which tends to simplify the processes of oxidation & reduction.

The ability of nanoparticles to break down MO while maintaining temperature under the influence of visible light exposure was used to measure their photocatalytic activity. Photo catalysts were added to a solution that already contained MO at concentrations of 5 ppm and 0.2 g/100 mL to increase its efficiency. In order for the dye molecule's adsorption and desorption by the photocatalytic surface to balance out, the solution was rapidly agitated for 30 mins while keeping it in a dark area. It was carried out in order to keep the recipe for the combination, a secret. In order to achieve the best possible balance, this step was done. The combination was subjected to visible light produced by a Tungsten filament lamp, which was directed at it from a distance of two to three inches. Aliquots of 9 to 10 mL were taken at regular intervals of 30 minutes while the reaction mixture was being constantly agitated. The results of centrifuging the mixture for three minutes at 6000 revolutions per minute are shown below. Because of the compound's ability to undergo quick charge recombination, it should not be shocking that photocatalytic activity for 2Co/BiO is lower compared to 3Co/BiO. This is because of the compound's ability to undergo rapid charge recombination.
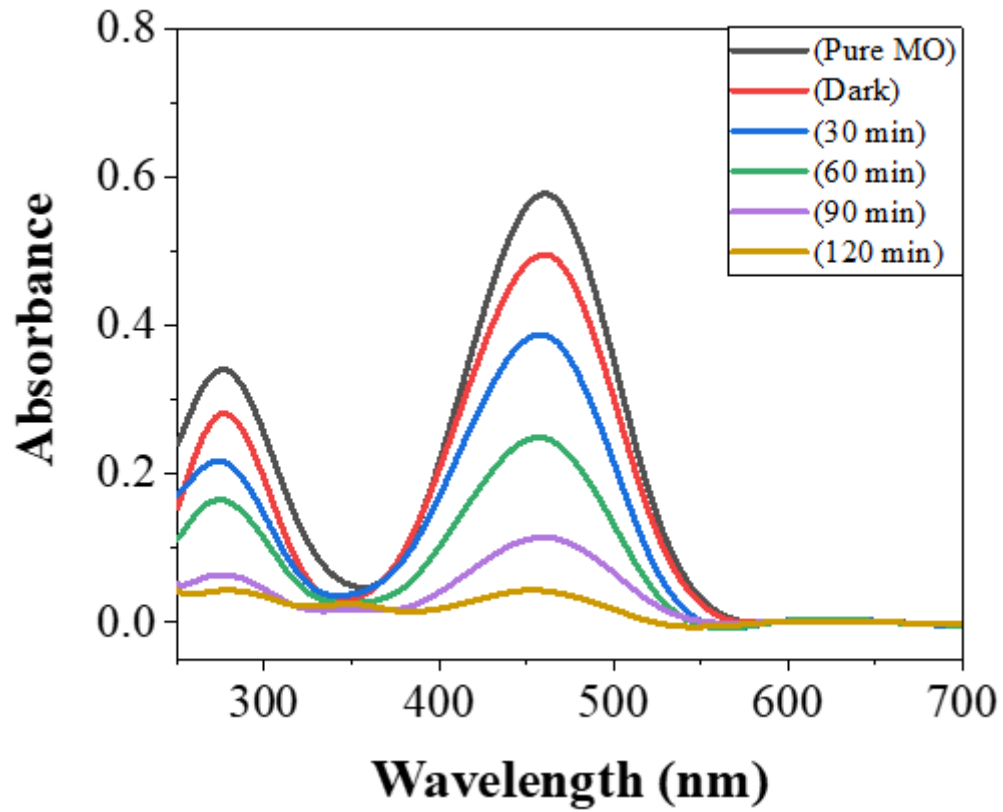
Figure 6 (a). Photocatalytic Degradation of MO Dye using 2 Percent Cobalt Dope Bismuth Oxide Nanoparticles
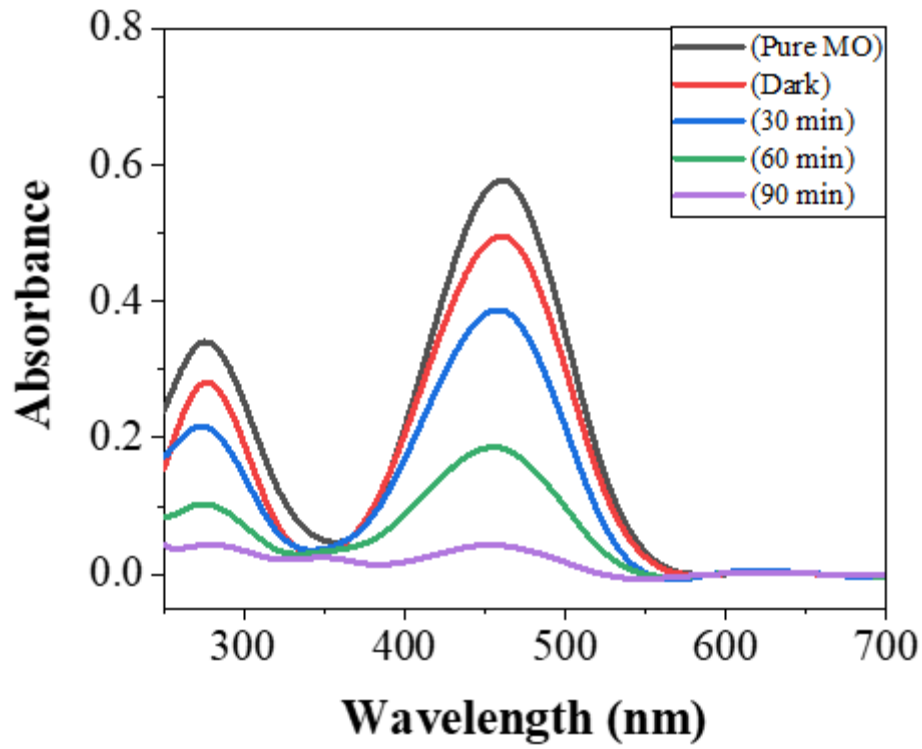
Figure 6(b). Photocatalytic Degradation of MO Dye using 3 Percent Cobalt Dope Bismuth Oxide NPs
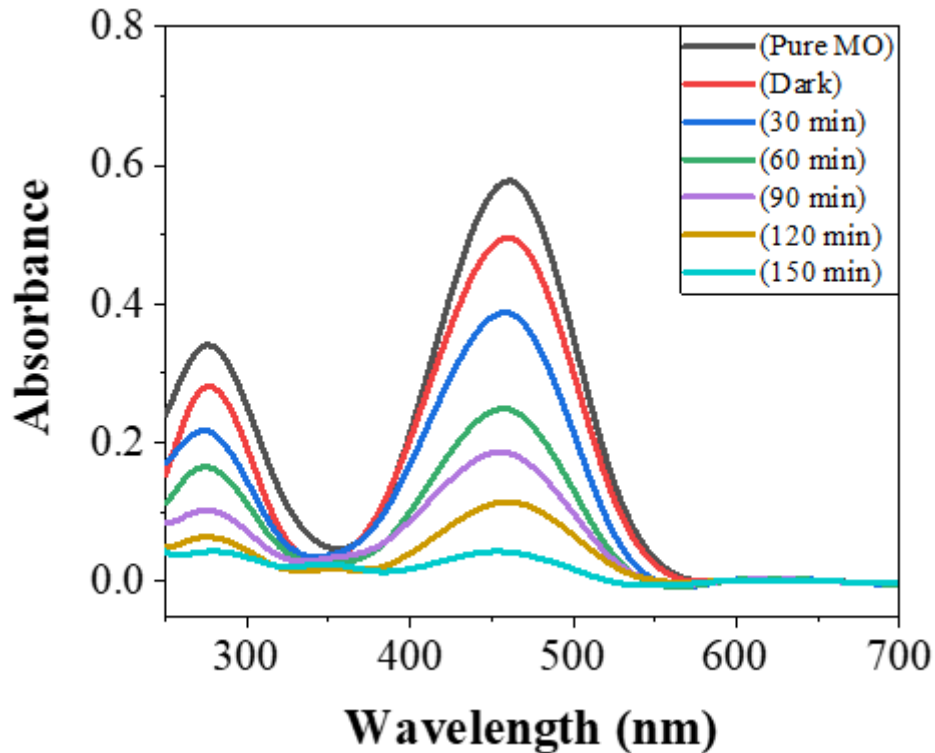
Figure 6(c). Photocatalytic Degradation of MO Dye using 3 Percent Cobalt Dope Bismuth Oxide NPs

The photocatalytic activities, on the other hand, are shown to considerably increase when extra cobalt is introduced as a dopant. In addition to this, the augmentation of photocatalytic degradation is directly related to the amount of cobalt dopant that is given, and the sample that is formed of 3Co/BiO has the highest potential for efficiency in terms of the degradation process. Yet, when there is a higher concentration of 4Co/BiO, the photocatalytic activity will decrease showed in fig 6 (a, b, and c). The silhouette effect is caused by cobalt, and not by any other substance. According to the findings of the photocatalytic degradation of MO, cobalt is an essential component for increasing the quantity of light that Bismuth Oxide nanoparticles (NPs) are able to absorb while simultaneously decreasing the rate of charge recombination that takes place within these particles.
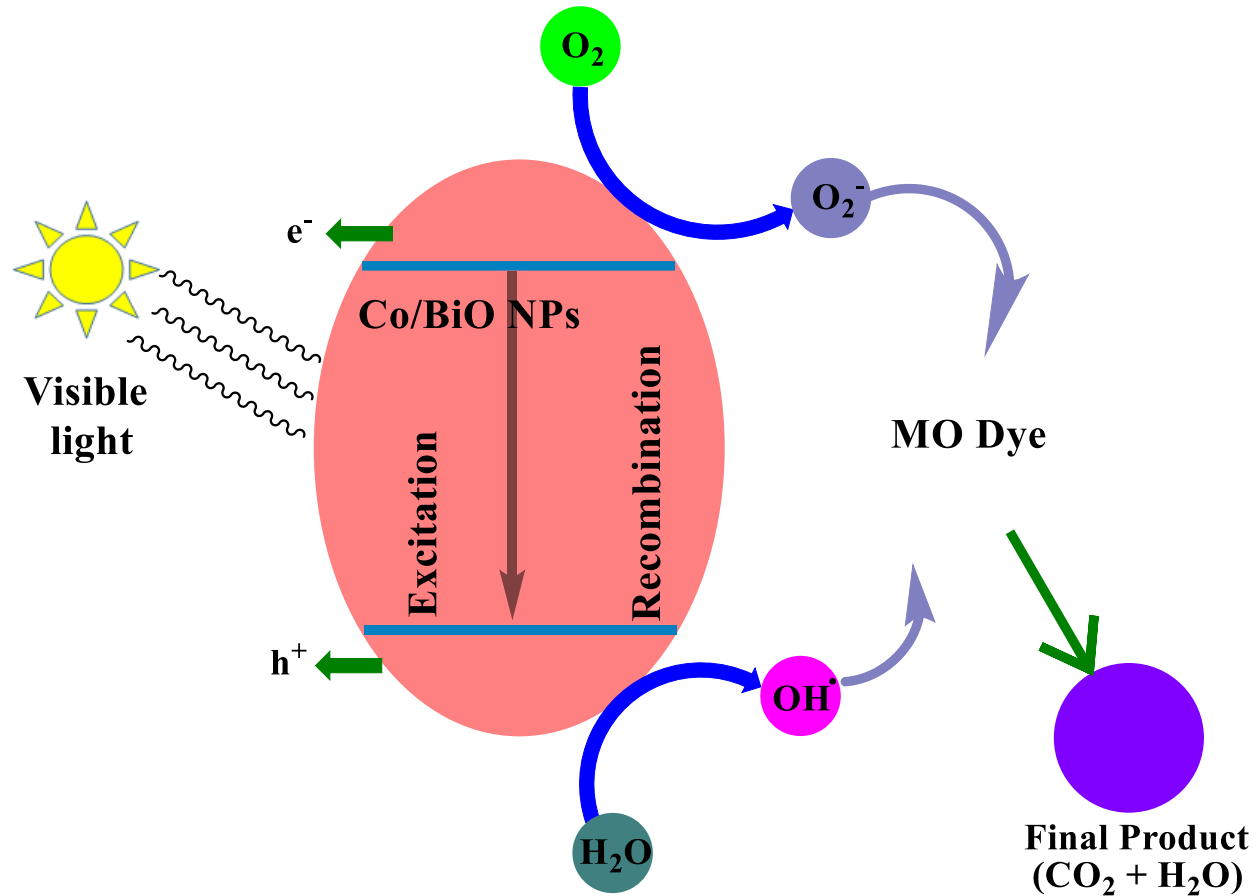
Figure 7. Photocatalytic MO dye degradation mechanism of Co/BiO NPs

The insertion of electrons back into the cobalt doped bismuth oxide NPs was caused by the MO dye's generation of reactive species in response to photon irradiation. When there was accessible oxygen in the solution, this contributed to the production of superoxide radicals, which sped up the photo degradation process. The dissolution of the chromophoric group and the transformation of the target dye into low molecular weight byproducts are both involved in the photocatalytic degradation of the dye. The primary cause of dye degradation is the production of electrons (e^-) and holes (h^+) on the catalyst surface when dyes are exposed to visible light. Water molecules mix with holes (h^+) to form the OH radical. Using intermediates HOO and H_2O_2, the O_2 molecule scavenges the electrons e and transfers them to OH. The powerful oxidizing species known as OH degrades the organic pigment non-selectively into H_2O, CO_2, and inorganic ions shown in fig 7. The job was carried out three times with the exact same experimental conditions,

and the standard deviation values were calculated each time. Fig 8 shows the MO dye's % degradation.
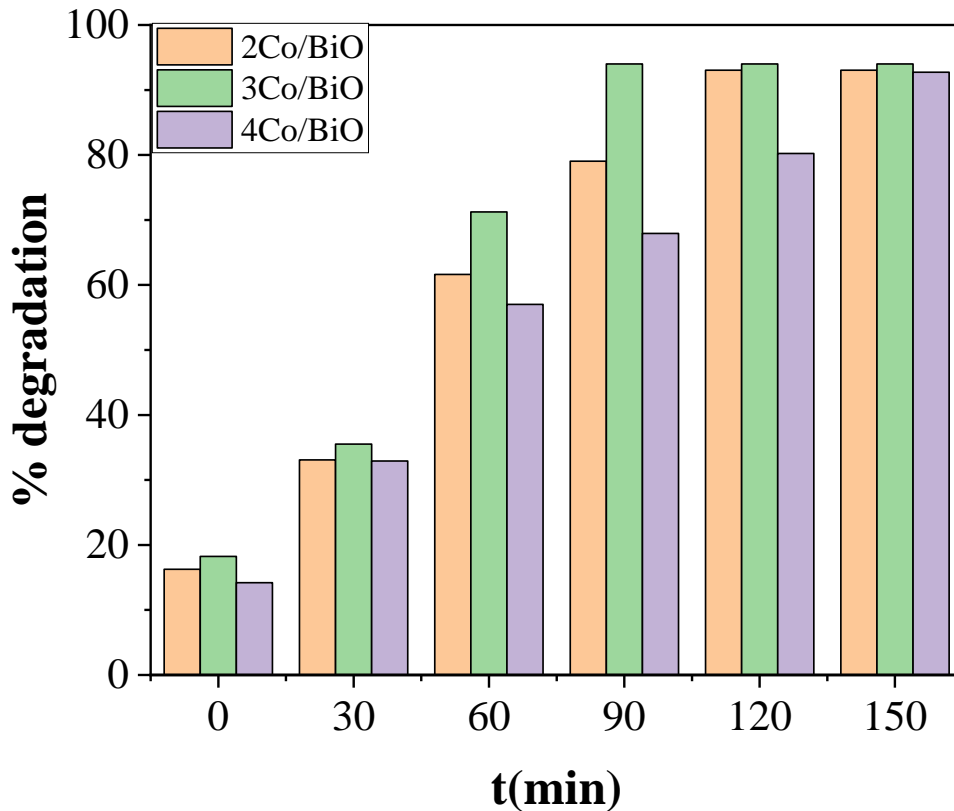

Figure 8. % Photocatalytic degradation of Cobalt dope Bismuth oxide NPs

4. Conclusion

We successfully synthesized Cobalt-doped Bismuth-oxide nanoparticles by hydrothermal method. We began by combining Cobalt chloride, Bismuth nitrate, Citric acid and Sodium hydroxide. Nanoparticles of cobalt-doped bismuth oxide with size less than 100 nm are categorized as metal nanoparticles. It is resistant to oxidation, chemically inert, and has magnetic characteristics. Various techniques, including UV-visible, FT-IR, XRD & SEM, were used for evaluating the optical properties, phase purity, & morphology of as-synthesized materials. The XRD analysis demonstrated that the composition of the generated systems was crystalline. Within the cobalt bismuth oxide composition, the vibratory modes were determined by analyzing

the FTIR spectra. The use of UV-visible bands made it possible to investigate the optical properties of Co/BiO NPs. It continued to determine if Co/BiO NPs photo catalysts could profitably remove Methyl Orange from water. The 3Co/BiO photo catalyst destroyed more than 94% of the MO dye, whereas the 2Co/BiO nanoparticles degraded around 93.04% of the MO dye and the 4Co/BiO nanoparticles degraded approximately 92.72% of the MO dye.

References

1.   Hamza, M., S. Muhammad, and S.J.A.S.A.P. Zahoor, *Biologically synthesized zinc oxide nanoparticles and its effect-a review.* 2022. **2**(9).

2.   Ali, A., *Synthesis of Silver Oxide Nanoparticles and its Antimicrobial, Anticancer, Anti-inflammatory, Wound Healing, and Immunomodulatory Activities-A Review.* Acta Scientific Applied Physics, 2023. **3**(7): p. 33-48.

3.   Kashif, M., et al., *Bismuth Oxide Nanoparticle Fabrication and Characterization for Photocatalytic Bromophenol Blue Degradation.*

4.   Ealia, S.A.M. and M. Saravanakumar. *A review on the classification, characterisation, synthesis of nanoparticles and their application.* in *IOP conference series: materials science and engineering.* 2017. IOP Publishing.

5.   Jarvie, H., King, Stephen and Dobson, Peter, *Nanoparticles.* 14 May. 2019.

6.   Fan, H., et al., *Photoinduced charge transfer properties and photocatalytic activity in Bi2O3/BaTiO3 composite photocatalyst.* 2012. **4**(9): p. 4853-4857.

7.   Raza, W., et al., *Synthesis, characterization and photocatalytic performance of visible light induced bismuth oxide nanoparticle.* 2015. **648**: p. 641-650.

8.   Liu, G., et al., *Synergistic effects of B/N doping on the visible-light photocatalytic activity of mesoporous TiO2.* 2008. **47**(24): p. 4516-4520.

9.   Blake, D.M., *Bibliography of work on the photocatalytic removal of hazardous compounds from water and air.* 1994, National Renewable Energy Lab., Golden, CO (United States).

10.   Singh, H., et al., *Heterogeneous photocatalysed degradation of 4-chlorophenoxyacetic acid in aqueous suspensions.* 2007. **142**(1-2): p. 374-380.

11.   Dass, S., et al., *Photocatalytic degradation of wastewater pollutants. Titanium-dioxide-mediated oxidation of polynuclear aromatic hydrocarbons.* 1994. **77**(1): p. 83-88.

12.   Ali, A.M., et al., *Doped metal oxide (ZnO) and photocatalysis: a review.* 2012. **40**(1): p. 11-19.

13.   Karunakaran, C., et al., *Preparation and characterization of antimicrobial Ce-doped ZnO nanoparticles for photocatalytic detoxification of cyanide.* 2010. **123**(2-3): p. 585-594.

14.   Akurati, K.K., et al., *Flame-made WO3/TiO2 nanoparticles: relation between surface acidity, structure and photocatalytic activity.* 2008. **79**(1): p. 53-62.

15.   Kubacka, A., M. Fernandez-Garcia, and G.J.C.r. Colon, *Advanced nanoarchitectures for solar photocatalytic applications.* 2012. **112**(3): p. 1555-1614.

16.   Herrmann, J.-M.J.T.i.c., *Heterogeneous photocatalysis: state of the art and present applications In honor of Pr. RL Burwell Jr.(1912–2003), Former Head of Ipatieff Laboratories, Northwestern University, Evanston (Ill).* 2005. **34**(1): p. 49-65.

17.   Zhang, X., et al., *Effect of aspect ratio and surface defects on the photocatalytic activity of ZnO nanorods.* 2014. **4**(1): p. 1-8.

18.   Yamashita, H., et al., *Photocatalytic degradation of organic compounds diluted in water using visible light-responsive metal ion-implanted TiO2 catalysts: Fe ion-implanted TiO2.* 2003. **84**(3-4): p. 191-196.

19.   Bettinelli, M., et al., *Photocatalytic activity of TiO2 doped with boron and vanadium.* 2007. **146**(3): p. 529-534.

20.   Lin, X., et al., *Photocatalytic activities of heterojunction semiconductors Bi2O3/BaTiO3: a strategy for the design of efficient combined photocatalysts.* 2007. **111**(49): p. 18288-18293.

21.   Kim, H.-i., et al., *Enhanced photocatalytic and photoelectrochemical activity in the ternary hybrid of CdS/TiO2/WO3 through the cascadal electron transfer.* 2011. **115**(19): p. 9797-9805.

22.   Patil, M., et al., *Synthesis of bismuth oxide nanoparticles at 100 C.* 2005. **59**(19-20): p. 2523-2525.

23.   Wang, Y., J. Zhao, and Z. Wang, *A simple low-temperature fabrication of oblique prism-like bismuth oxide via a one-step aqueous process.* Colloids and Surfaces A: Physicochemical and Engineering Aspects, 2011. **377**(1-3): p. 409-413.

24.   Gotić, M., S. Popović, and S.J.M.l. Musić, *Influence of synthesis procedure on the morphology of bismuth oxide particles.* 2007. **61**(3): p. 709-714.

25.   Monnereau, O., et al., *Synthesis of Bi2O3 by controlled transformation rate thermal analysis: a new route for this oxide?* 2003. **157**(1-4): p. 163-169.

26.   Skorodumova, N.V., et al., *Random conductivity of δ-Bi 2 O 3 films.* 2005. **86**(24): p. 241910.

27.   Gujar, T., et al., *Electrosynthesis of Bi2O3 thin films and their use in electrochemical supercapacitors.* 2006. **161**(2): p. 1479-1485.

28.   Zhang, L., et al., *Sonochemical synthesis of nanocrystallite Bi2O3 as a visible-light-driven photocatalyst.* 2006. **308**: p. 105-110.

29.   De Sousa, V.C., M.R. Morelli, and R.H.J.C.I. Kiminami, *Combustion process in the synthesis of ZnO–Bi2O3.* 2000. **26**(5): p. 561-564.

30.   Anilkumar, M., R. Pasricha, and V.J.C.i. Ravi, *Synthesis of bismuth oxide nanoparticles by citrate gel method.* 2005. **31**(6): p. 889-891.

31.   Yang, Q., et al., *Hydrothermal synthesis of bismuth oxide needles.* 2002. **55**(1-2): p. 46-49.

32.   Leontie, L., et al., *Structural and optical characteristics of bismuth oxide thin films.* 2002. **507**: p. 480-485.

33.   Fan, H., et al., *Optical properties of δ-Bi 2 O 3 thin films grown by reactive sputtering.* 2005. **87**(23): p. 231916.

34.   Ramamoorthy, R., P. Dutta, and S.J.J.o.m.s. Akbar, *Oxygen sensors: materials, methods, designs and applications.* 2003. **38**(21): p. 4271-4282.

35.   Eberl, J., H.J.P. Kisch, and P. Sciences, *Visible light photo-oxidations in the presence of α-Bi2O3.* 2008. **7**(11): p. 1400-1406.

36.   Han, M., et al., *m-BiVO 4@ γ-Bi 2 O 3 core–shell p–n heterogeneous nanostructure for enhanced visible-light photocatalytic performance.* 2013. **3**(47): p. 24964-24970.

37.   Wang, Y., et al., *Improved structural stability of titanium-doped β-Bi2O3 during visible-light-activated photocatalytic processes.* 2010. **45**(5): p. 1385-1392.

38.   Hameed, A., et al., *Synthesis, characterization and photocatalytic activity of NiO–Bi2O3 nanocomposites.* 2009. **472**(4-6): p. 212-216.

39.   Zhou, W., D. Jefferson, and J.J.J.o.S.S.C. Thomas, *A new structure type in the Bi2O3Nb2O5 system.* 1987. **70**(1): p. 129-136.

40. Castro, A., et al., *The new oxygen-deficient fluorite Bi3NbO7: synthesis, electrical behavior and structural approach.* 1998. **33**(1): p. 31-41.

41. Lazarraga, M., et al., *The cubic Bi1. 76U0. 12La0. 12O3. 18 mixed oxide: Synthesis, structural characterization, thermal stability and electrical properties.* 2005. **176**(29-30): p. 2313-2318.

42. Hameed, A., et al., *Photocatalytic activity of zinc modified Bi2O3.* 2009. **483**(4-6): p. 254-261.

43. Hameed, A., et al., *Surface phases and photocatalytic activity correlation of Bi2O3/Bi2O4-x nanocomposite.* 2008. **130**(30): p. 9658-9659.

44. Wu, S., et al., *Microemulsion synthesis, characterization of highly visible light responsive rare earth-doped Bi2O3.* 2012. **88**(5): p. 1205-1210.

45. Jian, Z., et al., *Microemulsion synthesis of nanosized TiO2 particles doping with rare-earth and their photocatalytic activity.* 2010. **86**(5): p. 1016-1021.